

# Biosorption of nitrate by thermodynamic and kinetics study using tamarind fruit shells

Murugesan S.R.<sup>1\*</sup>, Ganesan R.K.<sup>1</sup>, Sivakumar V.<sup>2</sup>, and Mani S.K.<sup>3</sup>

<sup>1</sup>Department of Civil Engineering, Dr.N.G.P. Institute of Technology, Coimbatore-641048, India

<sup>2</sup>Department of Civil Engineering, Hindusthan College of Engineering and Technology, Coimbatore-641032, India

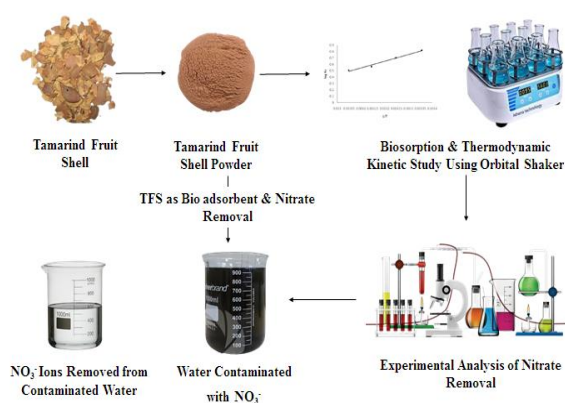
<sup>3</sup>Department of Agriculture Engineering, Kongunadu College of Engineering and Technology, Thottiam, Trichy-641048, India

Received: 11/09/2022, Accepted: 16/10/2022, Available online: 31/10/2022

\*to whom all correspondence should be addressed: e-mail: senthilcivilz@gmail.com

<https://doi.org/10.30955/gnj.004480>

## Graphical abstract



## Abstract

The majority of nitrate (NO<sub>3</sub><sup>-</sup>) pollutants come from a different type of industries. Even if present in low amounts, these nitrates are harmful to humans and aquatic systems. This research investigated the utilisation of Tamarind Fruit shell (TFS) as biosorbent in the removal of Nitrate from aqueous solution. TFS shell was modified by soaking it with distilled water. Many remediation strategies are available, but they are both costly and ineffectual. However, it has been discovered via significant research that waste materials such as tamarind bark, eggshells, and agricultural wastes are well suited to removing nitrate from wastewater using the biosorption process (Panida, *et al.*, 2010). Biosorption is a nitrate removal process that is both environment friendly and cost-effective. The equilibrium distribution of NO<sub>3</sub><sup>-</sup> onto the surface of the TFS can be best explained by Freundlich isotherm. Based upon the reaction of the thermodynamic study the TFS- NO<sub>3</sub><sup>-</sup> interaction is an endothermic (Amardeep, *et al.*, 2013). A substantial chance in the NO<sub>3</sub><sup>-</sup> - TFS interaction is expected because of the significant gain in the translational entropy by the displaced synchronised water molecules. Then the Chemiluminescence Analysing techniques Spectroscopic studies shows the biosorption capacity of TFS shows a

little variation between 1.25 mg/g for 1 mm size and 2.14 mg/g for 0.13 mm size.

**Keywords:** Biosorption, endothermic, Freundlich isotherm, entropy, TFS.

## 1. Introduction

Contamination of ground and surface waters with harmful pollutants such as inorganic anions, metal ions, synthetic xenobiotics, and others has resulted from India's and other countries continued industrial expansion and agricultural development (Sujatha, *et al.*, 2022). Biosorption has been shown to be a realistic alternative method for removing heavy metals from wastewater. Several natural and artificial hydrous solids have been investigated as biosorbent of heavy metals. (Panida Sampranpiboon and Pisit Charneitkong 2010) Among the umpteen inorganic species, nitrate (NO<sub>3</sub><sup>-</sup>) is of vital concern on global level, due to its universal in nature regarding human health (Islam and Patel, 2010). NO<sub>3</sub><sup>-</sup> gains contact in to the environment through various point and/or non-point sources such as agriculture and urban runoff, unsafe disposal of partially and untreated sewage and industrial wastes, leakage from septic tanks, landfill leachate, animal manure, and NO<sub>x</sub> air stripping waste from air pollution control devices, and others Owing to these effects, the WHO and IS: 10500, 1995 have set the respective maximum permissible limits of 50 and 45 mg/l for NO<sub>3</sub><sup>-</sup> in drinking water respectively An international environmental concern is the heavy metal pollution of aquatic systems that results from different industrial operations. The majority of industries in developing countries take very few or no steps to clean their wastewater before dumping it.

Since they are not biodegradable and can remain under various environmental circumstances, their presence in water bodies when it exceeds safe levels poses a major risk to people and the ecology (Praveen, *et al.*, 2021) As a result, it is crucial to rid the aquatic ecosystem of harmful contaminants in order to safeguard the environment and the general people. The focus is on the heavy metals chrome (VI) and iron (III) ions. Chromium is used in wood

preservation, textiles, antifouling agents in cooling towers, and chrome plating.

According to Hell *et al.*, (1998), BATs were rather costly and also face process in-situ complexity issues when treating groundwater directly. Amith Bhathagar and Milka Sillappar (2011) conducted a comprehensive analysis of various processes such as ion exchange, reverse osmosis, chemical techniques, and biological methods with respect to adsorption for possible consideration of sorption approach under BATs. Sorption of  $\text{NO}_3^-$  (concentrations between 1 and 1000 mg/l) from aqueous phase by utilizing powder activated carbon, untreated and/or treated coconut granular activated carbons, coconut shell or coconut husk activated carbon, carbon nanotubes, chitosan beads, sugarcane bagasse, alkaline lignin, cellulose, red mud, and many others have been successfully investigated, during the past one decade (Bhatnagar *et al.*, 2008; Chatterjee and Woo 2009). Due to the presence of suitable functional groups on their pore surfaces, the involvement of agricultural by-products in sorbing various hazardous anions and metal ions was widely established throughout the 1990s (Muhammad Imran Din, *et al.*, 2013). Simultaneously, the biosorption potential of Tamarind Fruit Shells (TFS) (a waste material after the processing of tamarind fruits) in sorbing  $\text{Cr}^{6+}$ , malachite green, chloropyriphos,  $\text{NO}_3^-$  and others, from past few years (Arivoli, *et al.*, 2012). Also, no particular literature concerning the use of TFS in eliminating  $\text{NO}_3^-$  from the aqueous phase exists as of yet, with the exception of research conducted by Prabhu (2012) in CMBR and FBR systems, respectively. The biosorbent can be characterised by X-ray Fluorescence spectroscopy (XRF) The thermodynamic and equilibrium distribution of  $\text{NO}_3^-$  onto the TFS, as well as the assessment of the rate-limiting phase, were done in this study (as a continuation of prior investigations) (Appunni, *et al.*, 2013)

Adsorption has thus become a successful method for cleaning up contaminants. Filtration, precipitation, reverse osmosis, adsorption, coagulation or flocculation, treatment with chlorine or hydrogen peroxide, bacterial cells, membrane systems, and ion exchange adsorption are some more methods used to treat water. As of now, adsorbents such as magnetite supported on cross-linked chitosan, mesoporous biochar, silica-coated magnetite spheres, activated carbon, and clay composites have been created and used. Recently, the adsorption of dyes and metal oxide by nanoparticles (NPs) has drawn considerable attention. Due to their porous architectures and huge specific surface areas, NPs shown potential efficiency.

## 2. Material and methods

### 2.1. Biosorbent

Tamarind Fruit Shells (TFS) was procured from the village near Bhavani town, Erode district, Tamil Nadu, India and pulverized to different sizes: i) passing through 1.41mm BIS sieve and retaining on 0.7 mm BIS sieve with a geometric mean size of 1 mm, ii) passing through 0.7 mm BIS sieve and retaining on 0.5 mm BIS sieve with a

geometric mean size of 0.6 mm and, iii) passing through 0.5 mm BIS sieve and retaining on 0.211 mm BIS sieve with a geometric mean size of 0.32mm, and iv) passing through 0.211 mm BIS sieve and retaining on 0.075 mm BIS sieve with a geometric mean size of 0.13 mm. To enhance the biosorption procedure, apply Response Surface Methodology (RSM). The powder is supposed to absorb the pollutants in its cavities (Biosorption) (Lenin *et al.*, 2021). The powder is extracted and filtered after being in the contaminated solution under agitation for 3 Hours. It was completely cleaned in distilled water to eliminate inessential contaminants, then oven dried for 10 hours at a temperature below  $110^\circ\text{C}$ , cooled in desiccators, and kept in sealed plastic containers (Raja *et al.*, 2022). Acidifying causes oxygen surface complexes which supposedly increase adsorption sites. Acidifying also is said to lead to an increase in surface area. All investigations, unless otherwise stated, employed a geometric mean size of 0.13 mm (Gokulan, *et al.*, 2021).

### 2.2. Chemicals

All chemicals and reagents were purchased from S.d Fine Chemicals Ltd in Mumbai, India, and were of AR grade. 1.6307 g of  $\text{KNO}_3$  (owing to its comparatively high solubility in distilled water compared to  $\text{NaNO}_3$ ) was dissolved in pyrogen-free doubly distilled water and then diluted according to the experimental conditions to make a stock solution of  $\text{NO}_3^-$  (1000 mg/l) (Meng Xue Xiong, *et al.*, 2022) The average pH of the distilled water was 6.6, and the electrical conductivity was less than 10 mho/cm. The chemicals utilised were of the analytical grade and were obtained from Merck (Germany) and the Sigma-Aldrich Company (U.S.A.).  $\text{MgCl}_2 \cdot 6\text{H}_2\text{O}$ ,  $\text{NaOH}$ , ammonium hydroxide ( $\text{NH}_4\text{OH}$ ) (28–30% $\text{NH}_3$ ), iron sulphate hexa-hydrate ( $\text{FeSO}_4 \cdot 7\text{H}_2\text{O}$ ), zinc nitrate (Kumar *et al.*, 2022).

### 2.3. Methods

#### 2.3.1. Analysis of $\text{NO}_3^-$

The  $\text{NO}_3^-$  was analysed by double beam UV-VIS Spectrophotometer with 10 mm path length high quality quartz cuvettes at a wavelength of 220 nm $\lambda$ . The concentration of  $\text{NO}_3^-$  in the aqueous phase was assessed by using the standard graph (linear plot of absorbance versus concentration of  $\text{NO}_3^-$ ) as shown in Figure 1. Also, as per Prabhu (2012), the interference caused by leaching of organic matter from TFS at 220 nm $\lambda$  was appropriately taken into account by measuring its absorbance at 275 nm $\lambda$ . The experimental errors were below 4%.

#### 2.3.2. Characterisation of Biosorbent

The physicochemical characteristics of the TFS were determined as per the standard methods followed by Stadler *et al.*, 2008 and are shown in Table 1. Also, the specific surface area ( $\text{m}^2/\text{g}$ ) and BET surface area ( $\text{m}^2/\text{g}$ ) are measured by Filtrasorb-II:2300 and the pH of zero-point charge ( $\text{pH}_{zpc}$ ) was analyzed by the instrumental method and standard titrimetric method (Gokulan, *et al.*, 2019). With the Non-Local Density Functional Theory (NLDFT) and the assumption of a cylindrical pore shape, the pore size distribution was determined from the

adsorption branch. (Gokulan *et al.*, 2014) These results are shown in Table 2. Although the TFS' precise properties and functional groups have been published elsewhere (Popuri *et al.*, 2007), the SEM and FTIR findings are still being tested targeting for lead contamination in industrial wastewater (India), and therefore want to prepare synthetic lead nitrate solution accordingly.

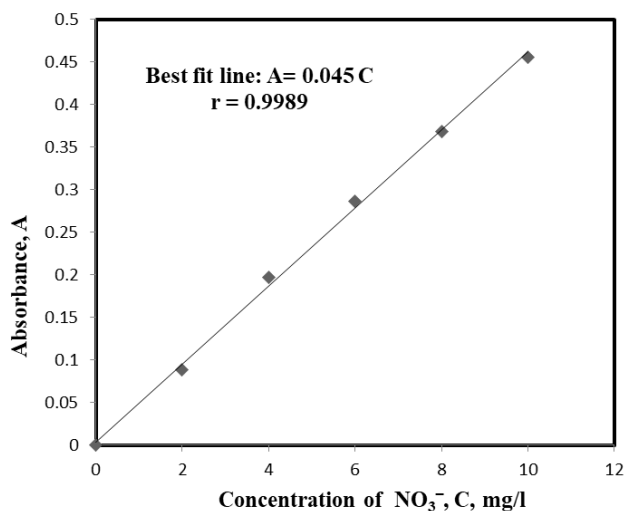


Figure 1. Calibration Curve for NO<sub>3</sub><sup>-</sup> Analysis

### 2.3.3. Biosorption Studies

All biosorption experiments were carried out in a CMBR system using either distilled or tap water at room

temperature. The biosorption of NO<sub>3</sub> was assessed using a jar test device with 6 flat blade stirrers (each 7.6 x 2.5 cm<sup>2</sup>) operated by a 0.05 HP motor with an induced speed range of 10 to 400 rpm (Figure 2). All of the studies were conducted in 1L Borosil glass beakers holding 300 mL of prepared NO<sub>3</sub> solution equating to a liquid depth of 3.5 cm and a preset dosage of biosorbent.

### 2.3.4. Kinetics Studies

For the assessment of equilibrium time in CMBR, the biosorption kinetics were individually studied for each dosage of TFS (2, 4, 6, 8, and 10 g/l) of geometric mean size of 0.13mm; for an initial concentration of 70mg/l, at a pH of 5, and under an agitation speed of 100 rpm (Jegan *et al.*, 2020). The Brunauer-Emmett-Teller (BET) theory seeks to explain how molecules physically adhere to a solid surface. Similarly, separate kinetics tests were carried out for different diameters of TFS (1, 0.6, 0.32, and 0.13mm) as well as varied starting concentrations of 100, 70, 40, and 10 g/l.

### 2.3.5. Interruption test

The rate-limiting stage of the biosorption process was assessed using the multiple interruption test established by (Shankhamala *et al.*, 2021). The TFS was removed from the reaction mixtures one or more times and then reintroduced after a 5-minute interruption interval. NO<sub>3</sub><sup>-</sup> was measured at the conclusion of each response time period (Gokulan, *et al.*, 2019).

Table 1. Physiochemical Characteristics of the TFS

Sl. No.	Parameter	Result (average of triplicate results)
1	pH	3.98
2	Specific gravity	1.25
3	Bulk density, kg/m <sup>3</sup>	0.54 – 0.58
4	Porosity (mechanical)	0.25 – 0.30
5	Loss of weight after washed with 4 l (200 ml x 20) of distilled water, %	3
6	Dissolved organic matter from TFS, %	1.1
7	Ash content, %	6.5

Table 2. Size, Surface Areas and pH<sub>zpc</sub> of TFS

S.No	TFS size, mm		Approximate No. of particles per 10 mg <sup>2</sup>	Specific Surface area*, m <sup>2</sup> /g	BET surface area*, mg/g	pH <sub>zpc</sub> *	
	Geometric mean size	Spherical equivalent				Instrument based	Titrimetric Based
1	0.13	0.16	2445 ± 10	34.1	76.4	4.62	4.84
2	0.32	0.38	405 ± 8	26.3	74.6	4.63	4.72
3	0.6	0.72	85 ± 3	24.6	69.1	4.61	4.81
4	1	1.2	25 ± 1	20.8	62.9	4.65	4.75

### 2.3.6. Equilibria Studies

The goal of the biosorption equilibrium investigation was to learn more about the nature of the NO<sub>3</sub><sup>-</sup> equilibrium distribution on the biosorbent and in the liquid phase. The general equilibria experiments were carried out for

different diameters (1, 0.6, 0.32, and 0.13 mm) in the concentration range of 10 to 100 mg/l of NO<sub>3</sub><sup>-</sup>, at a TFS dosage of 10 g/l, agitation speed of 100 rpm, pH of 5, contact period of 3 h, and at room temperatures. For the thermodynamic relationship between NO<sub>3</sub><sup>-</sup> and TFS,

equilibria studies were conducted for five temperatures: 20, 30, 40, 50, and 60 °C, at a TFS dose of 10 g/l, pH of 5, contact time of 3 h, agitation speed of 150 rpm (Orbital Shaker- cum- Incubator, Neolab, India), and NO<sub>3</sub> concentrations ranging from 10 to 100 mg/l.

### 3. Results and discussion

#### 3.1. Reliability of TFS in Removing NO<sub>3</sub><sup>-</sup>

Although the biosorption of numerous anionic hazardous species is mostly dependent on the biomaterial's properties, its dependability should also be examined in light of the marginal differences that might exist between materials gathered in different places. TFS is widely available in various regions of Tamilnadu (as indicated in literature), and it was gathered for this study in a place other than those mentioned in prior studies (Rao and Puttanna, 2000; Demiral *et al.*, 2010; Prabhu, 2012).

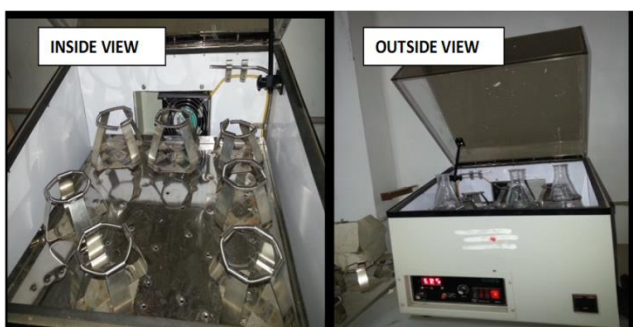


Figure 2. Photograph Showing the Orbital Shaker used for Equilibria and Thermodynamic Studies

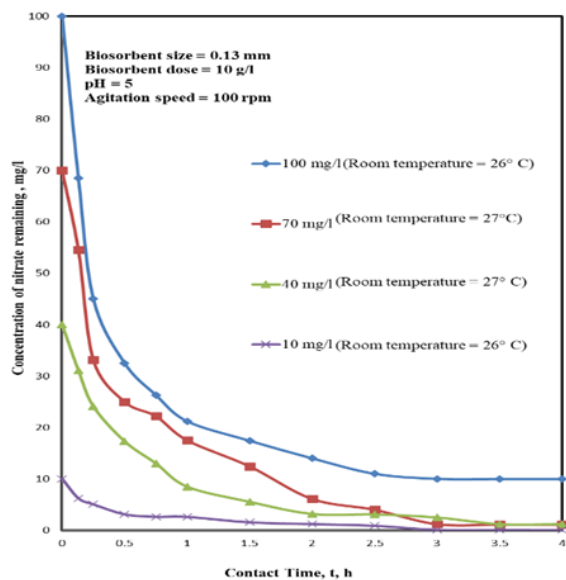


Figure 3. Biosorption Kinetics Profiles of NO<sub>3</sub><sup>-</sup> by TFS.

As a result, a TFS biosorption of NO<sub>3</sub> reliability investigation was carried out. According to Cengeloglu *et al.*, (2006) reliability study, the biosorption capacity of TFS is highly dependent on the source or origin of TFS. In addition, there was a 10% difference between the Perundurai-based TFS and the Bhavani-based TFS in this study. This is because to the minor morphological differences that the various TFSs may have exhibited.

However, targeting for lead contamination in industrial wastewater (India), and therefore want to prepare synthetic lead nitrate solution accordingly across the numerous TFSs collected in different regions of Tamilnadu, a 10-15% variance in NO<sub>3</sub><sup>-</sup> biosorption might be predicted.

#### 3.2. Assessment of sorption equilibrium time in CMBR

Solute absorption in the CMBR is quick initially, then slows down as it approaches saturation. The sorption rate is larger than the desorption rate during quick stage sorption, and as time passes, the disparity between the rates gradually narrows until they appear to be equal (Hariprasad and Geresh, 2009). Equilibrium time is defined as the point at which the sorption and desorption rates appear to be equal. The fluctuation of sorbate removal with respect to elapsed time is predicted to follow a curvilinear pattern in CMBR, and the equilibrium time can range from a few minutes to many days. Because operating the system for a long period is difficult and cumbersome, the equilibrium time is chosen so that no significant occurs beyond this time, i.e., the curve (removal vs time) is nearly asymptotic to the time axis (Priya, *et al.* 2020). The choice of the equilibrium period, on the other hand, is largely determined by system factors such as the initial sorbate concentration, sorbent dosage, and sorbent size. To further understand the influence of these factors on equilibrium time, kinetic experiments were done.

#### 3.3. Evaluation of biosorption equilibrium time

Figures 3-8 demonstrate the fluctuations in NO<sub>3</sub><sup>-</sup> concentrations over time for various factors. The NO<sub>3</sub><sup>-</sup> removal efficiencies (percent) at various periods were computed using these s.

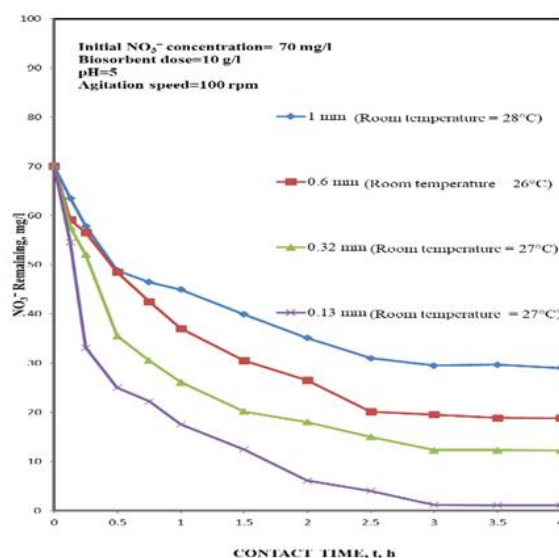


Figure 4.

#### 4. Effect of Biosorbent Size on Biosorption of NO<sub>3</sub><sup>-</sup> by TFS

However, after looking at the graphs, any figure between 2.5 and 4 h for the equilibrium time might be proposed. To get over this issue, a logical technique based on two separate criteria (Bhargava and Killedar, 1991) was used to calculate a precise equilibrium period. The criteria are: i) based on the arbitrary cutoff value of the slope (3%) of

the variation curve and ii) based on the arbitrary termination point of 95% of maximum removal, for chosen variable. The equilibrium time (from criterion I) was estimated, for each of the variable.

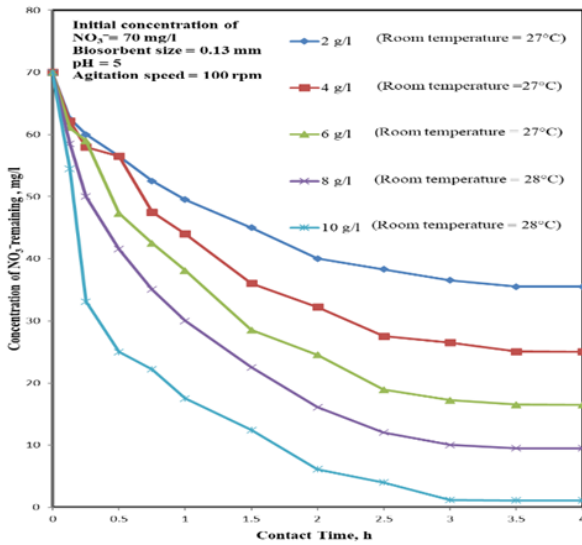


Figure 5. Effect of Biosorbent Dose on Biosorption of  $\text{NO}_3^-$  by TFS

Figures 3-8 demonstrate the fluctuations in  $\text{NO}_3^-$  concentrations over time for various factors. The  $\text{NO}_3^-$  removal efficiencies (percent) at various periods were computed using these s. However, after looking at the graphs, any figure between 2.5 and 4 h for the equilibrium time might be proposed. To get over this issue, a logical technique based on two separate criteria (Bhargava and Killedar, 1991) was used to calculate a precise equilibrium period. The criteria are: i) based on the arbitrary cutoff value of the slope (3%) of the variation curve and ii) based on the arbitrary termination point of 95% of maximum removal, for chosen variable. The equilibrium time (from criterion I) was estimated, for each of the variable.

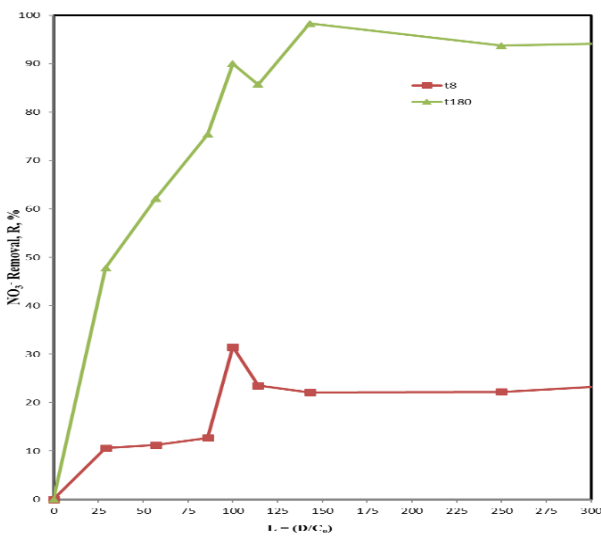


Figure 6. Variation of  $\text{NO}_3^-$  Removal with respect to L for  $t_3$  and  $t_{180}$

3.4. Determination of Rate Limiting Step

There are essentially three consecutive mass transport steps associated with the sorption of solutes from the solution by porous sorbents. Figure 9 shows a schematic representation of them. Film transport is the second stage, which involves solute diffusion across a hypothetical "film" or hydrodynamic boundary layer. Except for a small amount of sorption that occurs on the exterior surface of the sorbent during third and final step, the solute then must diffuse within the pore volume of the sorbent and/or along pore-wall surfaces to an active sorbent sizes (pore diffusion) (Crittender and Weber, 1978). Because they act in series, the slower of the two steps will be rate limiting (Benfield *et al.*, 1982).

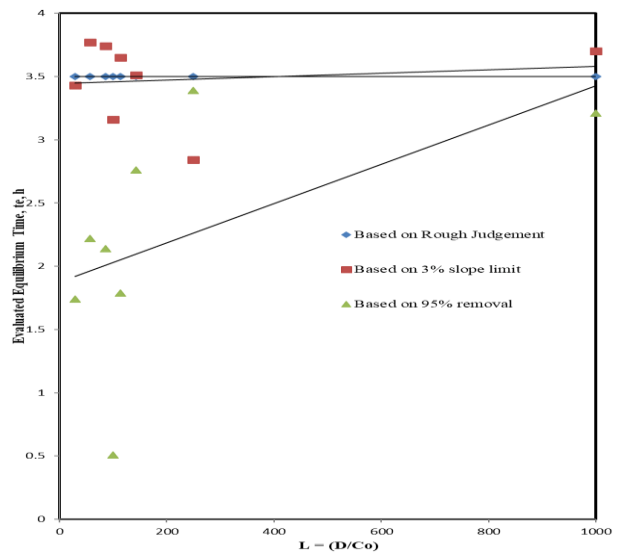


Figure 7. Variation of Equilibrium Time vs  $D/C_0$

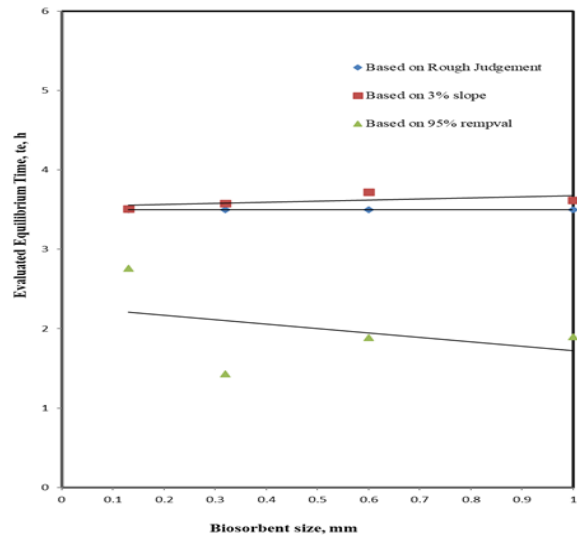


Figure 8. Variation of Equilibrium Time vs Biosorbent Size

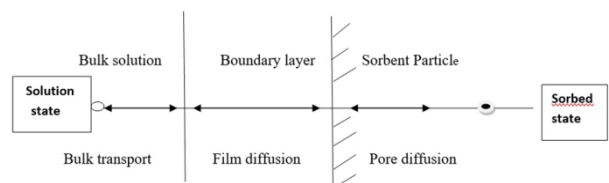


Figure 9. Mass Transport Steps in Sorption by Porous Sorbents

3.5. Interruption Test

The kinetics profiles of both interruption and non-interrupted tests are shown in Figure 10. Pore diffusion is the rate-limiting phase in both rapid and slow biosorption zones, according to the multiple interrupted testing curve (i.e., because of the substantial deviations between the uninterrupted and interrupted kinetics profiles, as per Zogorseki *et al.*, 1976).

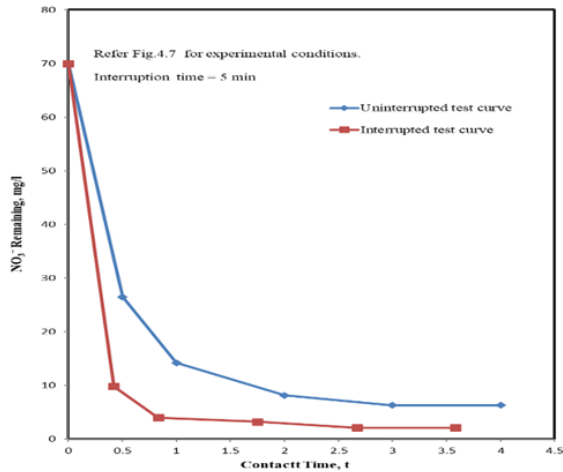


Figure 10. Kinetics Profiles of NO<sub>3</sub><sup>-</sup> Biosorption by TFS – Interruption and Uninterruption Tests

3.6. Effects of temperature and thermodynamic parameters

The Freundlich sorption isotherms at various temperatures are given in Figure 11. Although K<sub>f</sub> values rose as the temperature of the solution increased, the degree of attachment (reduction in 1/n values) fluctuated as the temperature of the solution grew. Further, the effect of temperature can be illustrated by using thermodynamic parameters like, changes in the energy ( $\Delta G^0$ ), enthalpy ( $\Delta H^0$ ), entropy ( $\Delta S^0$ ).

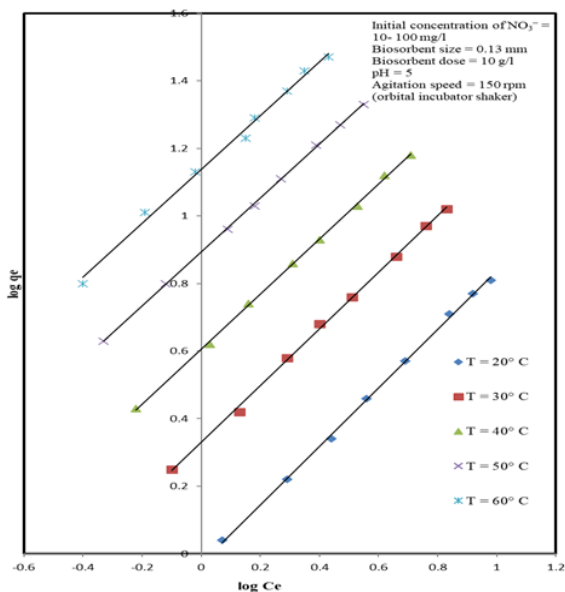


Figure 11. Freundlich Sorption Isotherm for Different Temperatures

Where, K<sub>0</sub> is a thermodynamic equilibrium constant for biosorption process, determined from the plot of lnq<sub>e</sub>/C<sub>e</sub> vs q<sub>e</sub> (Figure 12) and extrapolating to zero q<sub>e</sub>, as per the graphical procedure explained elsewhere (Khan and Singh, 1987). A linear plot of ln K<sub>0</sub> vs 1/T (Figure 13) was obtained and  $\Delta H^0$  (59.32 kJ/ mol) and  $\Delta S^0$  (201.95 J/K mol) were determined. The endothermic nature of NO<sub>3</sub><sup>-</sup> biosorption was reflected by (i) the positive values of  $\Delta H^0$  and (ii) the decreasing values of  $\Delta G^0$  with increasing temperature. The high randomness at the solid/solution and greater affinity of NO<sub>3</sub><sup>-</sup> to TFS, during biosorption, is revealed by high values of  $\Delta S^0$ . Also, the increased randomness in the NO<sub>3</sub><sup>-</sup> - TFS interaction was due to significant gain in the transitional entropy by the displaced coordinated water molecule than is lost by NO<sub>3</sub><sup>-</sup> species (Unnathan and Anirudhan, 2001).

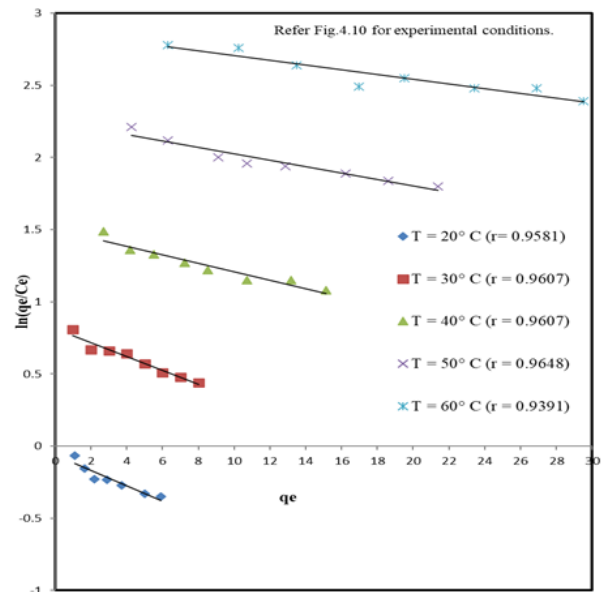


Figure 12. Plot of ln(q<sub>e</sub>/C<sub>e</sub>) vs q<sub>e</sub> at Different Temperatures for Removal of NO<sub>3</sub><sup>-</sup> by TFS

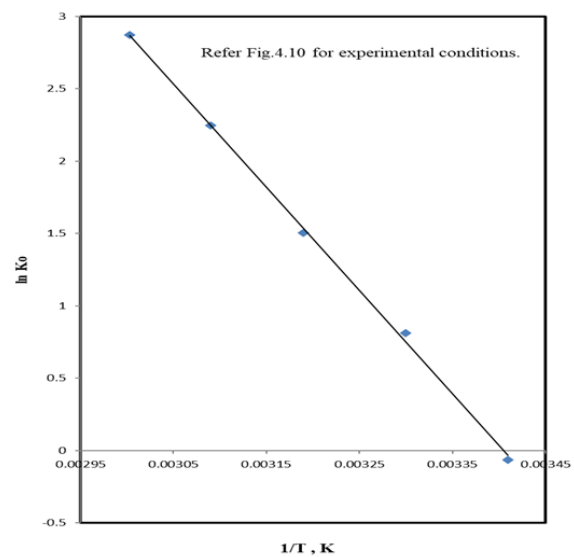


Figure 13. Plot of ln (K<sub>0</sub>) vs 1/T

For this purpose, the equilibrium concentration (C<sub>e</sub>) at constant amount of sorbed NO<sub>3</sub><sup>-</sup> was obtained from the sorption isotherm data at different temperatures (Figure

14). From the plot of  $\ln C_e$  vs  $1/T$  (Figure 14),  $\Delta H_x$  were calculated for different amount of  $\text{NO}_3^-$ . These values are respectively 61.09, 60.12, 54.64, 59.23, and 59 kJ/mol for the loadings of 5, 10, 20, 25, and 30 mg/g surface loadings. In the experiments, we obtain equilibrium concentration for any initial concentration after the equilibrium time ( $t_e$ ). then ascertain  $q_e$ 's value. Plotting  $C_e/q_e$  on the y-axis and  $C_e$  on the x-axis then allows the Langmuir isotherm model to be solved. The variation of  $\Delta H_x$  with the surface loading is shown in Figure 15, which indicates that TFS possess heterogeneous surface with effective lateral interaction between sorbed  $\text{NO}_3^-$  species.

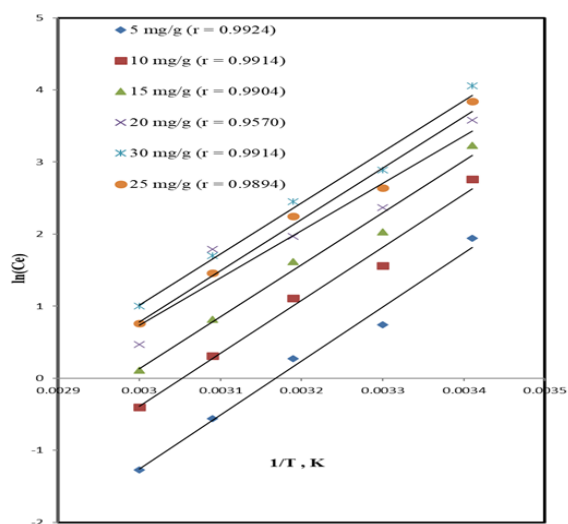


Figure 14. Plots of  $\ln C_e$  vs  $1/T$  for Constant Biosorption of  $\text{NO}_3^-$

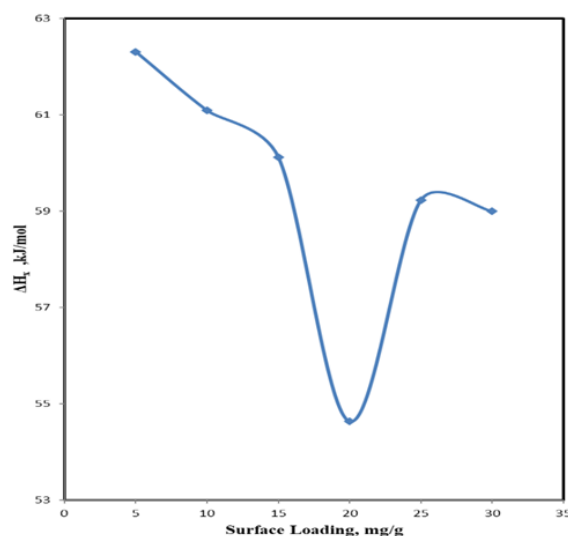


Figure 15. Variation of  $\Delta H_x$  with respect to Surface Loading

#### 4. Conclusion

The Tamarind Fruit Shells, a waste material from natural environment, was converted into a biosorbent, which show good sorption for the elements studied. This material can be used for the removal of these essentials from the liquid effluent after optimisation of different physico-chemical parameters of the effluent. Based on the investigation pertaining to "Thermodynamic and

Equilibrium Biosorption of  $\text{NO}_3^-$  by Tamarind Fruit Shells", the following conclusions are drawn. The TFS is a good biosorbent in eliminating  $\text{NO}_3^-$  from aqueous phase. The TFS is highly suitable in CMBR system. The TFS dose and initial  $\text{NO}_3^-$  concentration will highly influence the attainment of equilibrium time when compared to the size of TFS. The rational approach is most appropriate than the rough judgement, for the assessment of equilibrium in CMBR. Based on the interruption tests, pore diffusion is the rate limiting in the entire biosorption kinetics. The equilibrium distribution of  $\text{NO}_3^-$  onto the surface of the TFS can be best explained by Freundlich isotherm, due to the fact that the experimental data's  $R^2$  value fits the Freundlich Isotherm appropriately. The natural log of the negative intercept instead of the Freundlich constant  $k$  ( $\ln k$ ). It's acceptable to be unfavorable. Calculate  $\exp(-0.7585)$  to find  $k$ , and you'll receive a consistent positive Freundlich capacity constant. Also, the biosorptive capacity of TFS shows a little variation between 1.25 mg/g for 1 mm size and 2.14 mg/g for 0.13 mm size. The TFS -  $\text{NO}_3^-$  interaction is an endothermic process. Based on the cost analysis and the absorption period, the biosorption process is also evaluated. A high randomness at the solid/solution and greater affinity of  $\text{NO}_3^-$  to TFS is expected during biosorption. Using the Brunauer-Emmett-Teller (BET) theory, the adsorption property can be ascertained. A substantial randomness in the  $\text{NO}_3^-$  - TFS interaction is expected because of the significant gain in the translational entropy by the displaced coordinated water molecules.

#### Declarations

**Ethical approval:** Not applicable

**Consent to participate:** Not applicable

**Consent for publication:** Not applicable

**Funding:** Not applicable

**Competing interests:** The authors declare no competing interests.

**Availability of data and materials:** All data generated or analyzed during this study are included in this published article.

#### References

- Arivoli S., Marimuthu V., Ravichandran T. and Hema Kinetic M. (2012). Equilibrium and mechanistic studies of nickel adsorption on a low cost activated calcite powder. *Indian Journal of Science and Technology*, **1**(1), 41–49.
- Benfield L.D., Judkins J.F., and Weand V.L. (1982). *Process Chemistry for Water and Wastewater Treatment*. Printce-Hall, Inc, NJ.
- Bhargava D.S., and Killedar D.J. (1991). Judgement of equilibrium time during adsorption-a rational approach. *Indian Journal of Environmental Health*, **33**(4), 464-489.
- Bhatnagar A., and Sillappr M. (2011). A Review of emerging adsorbents for nitrate removal from water. *Chemical Engineering Journal*, **168**, 493.
- Bhatnagar A., Ji M., Choi Y.H., Jung W., Lee S.H., Kim S.-J., Lee G., Suk H., Kim H.S., Min B., Kim S.H., Jeon B.H., and Kang J.W.

- (2008). Removal of nitrate from water by adsorption onto zinc chloride treated activated carbon. *Separation Science Technology*, **43**, 886.
- Cengeloglu Y., Tor A., Ersoz M., and Arslan G. (2006). Removal of nitrate from aqueous solution by using red mud. *Separation and Purification Technology*, **51**, 374.
- Chatterjee S.n and Woo S.H. (2009), Nitrate removal from aqueous solutions by chitosan hydrogel beads. *Journal of Hazardous Materials*, **164**, 1012.
- Crittender J.R., and Weber J. (JR). (1978). Predictive model for desine of fixed bed adsorbers, in parameter estimation and model development. Journal of Environmental Engineering Division, Ac, 185.
- Demiral.P, and Gunduzoglu G. (2010), Removal of nitrate from aqueous solutions by activated carbon prepared from sugar beet bagasse, *Bioresour. Technol.* 101 1675–1680.
- Din M.I., Mirza M.L., and Ata S. (2013). Thermodynamics of biosorption for removal of Co(II) ions by an efficient and ecofriendly biosorbent (Saccharum bengalense): Kinetics and Isotherm Modeling, Hindawi Publishing Corporation. *Journal of Chemistry*, Article ID 528542, 11 pages
- Ghosh S., Sarkar A., and Nayek H.P. (2021). Elucidation of selective adsorption study of Congo red using new Cadmium(II) metal-organic frameworks: Adsorption kinetics, isotherm and thermodynamics. *Journal of Solid State Chemistry*, **296**, 121929
- Gokulan R., Ganesh Prabhu G., and Jegan J. (2019). A novel sorbent Ulva lactucaderived biochar for remediation Remazol brilliant orange 3R in packed column. *Water Environment Research*, **91**(7), 642–649.
- Gokulan R., Kalyani G., and Killi S. (2022). Removal of reactive Red 120 in a batch technique using seaweed-based biochar: a response surface methodology approach. *Journal of Nanomaterials, Hindawi Publications*, **2022**, Article ID 7604383. <https://doi.org/10.1155/2022/3621807>, (Indexed in SCI, I.F: 3.79, Q2).
- Gokulan R., Pradeepkumar S., and Elias G. (2021). Continuous sorption of remazol brilliant orange 3R using Caulerpa scalpelliformis Biochar. *Advances in Materials Science and Engineering*, **2021**, Article ID 6397137, 7 pages.
- Hariprasad C.P., and Geresh M. (2009). Biosorption of Malachite Green from Aqueous Phase by CMBR and FBR. Proceedings of National Conference on Innovations in Civil Engineering, ICE'09.
- Hell F., Lahnsteiner J., Frischherz H., and Baumgartner G. (1998). Experience with full scale electro dialysis for nitrate and hardness removal. *Desalination*, **117**, 173.
- Heviraab L., Zilfac, Joshua R., Ighaloef O., and Zeina R. (October 2020). Biosorption of Indigo Carmine from aqueous solution by Terminalia Catappa shell. *Chemical Engineering*, **8**(5), 104290.
- Huang and Ostovic. (1978). Removal of cadmium (II) by activated carbon adsorption. *American Society of Civil Engineers*, **104**(5).
- IS: 10500. (1995). Drinking Water Standards of India.
- Islam R., and Patel M. (2010). Synthesis and physicochemical characterization of Zn/Al chloride layered double hydroxide and evaluation of its nitrate removal efficiency. *Desalination*, **256**, 120–128.
- Jalali M. (2005). Nitrates leaching from agricultural land in Hamadan, Western Iran. *Agricultural Ecosystem Environment*, **110**, 210.
- Jegan J., Praveen S., Bhagavathi Pushpa T., and Gokulan R. (2020). Sorption kinetics and isotherm studies of cationic dyes by arachis hypogaea shell derived biochar as low-cost adsorbent. *Applied Ecology and Environmental Research*, **18**(1), 1925–1939.
- Khan A.A., and Singh R.P. (1987). Adsorption thermodynamic of carbon furan on Sn(IV) Arsenosilicate in H<sup>+</sup>, Na<sup>+</sup>, and Ca<sup>2+</sup> forms. *Colloids Surface*, **24**, 33–42 (1987).
- Kumar M., Sujatha S., Gokulan R., Vijayakumar A., Praveen S., and Elayaraja S. (2021). Prediction of RSM and ANN in the remediation of Remazol Brilliant Orange 3R using biochar derived from Ulva Lactuca. *Desalination and Water Treatment*, **211**, 304–318.
- Lenin Sundar M., Kalyani G., Gokulan R., Ragunath S., and Joga Rao H. (2021). Comparative adsorptive removal of Reactive Red 120 using RSM and ANFIS models in batch and packed bed column. *Biomass Conversion and Biorefinery*.
- Popuri S.R., Jammala A. and Abburi K. (2007). Biosorption of Hexavalent Chromium using Tamarind (Tamarind indica) Shell- a Comparative Study. *Electronic Journal of Biotechnology*, **10**(3), 1.
- Prabhu (2012) 'Biosorption of Nitrate onto Tamarind Fruit Shells', M. E Thesis Submitted to Anna University (Coimbatore), Coimbatore.
- Praveen S., Gokulan J Jegan, T Bhagavathi Pushpa, Techno-economic feasibility of biochar as biosorbent for basic dye sequestration, Journal of Indian Chemical Society.
- Priya A.K., Gokulan R., Vijay Kumar A., and Praveen S. (2020). Biodecolorization of remazol dyes using biochar derived from Ulva reticulata: Isotherm, kinetics, desorption and thermodynamic studies. *Desalination and Water Treatment*, **200**, 286–295.
- Raja Murugadoss J., Balasubramaniam N., Gokulan R., Naga Rajesh K., Pandian Sreelal G., Arti Sudam P., Zunaithur Rahman D.R., and Nasar Ali R. (2022). Optimization of river sand with spent garnet sand in concrete using RSM and R programming packages. *Journal of Nano Materials, Hindawi Publications*, **2022**, Article ID 4620687.
- Rao E.V.S.P. and Puttanna K. (2000), Nitrates, Agriculture and Environment, *Curr. Sci.* 79, 1163.
- Ravindiran G., Elayaraja S., Navaneethan P., Rajeshkannan R., and Abinaya S. (2014)., Assessment of physicochemical characteristics of municipal wastewater by microalgae. *International Journal of ChemTech Research*, **6**(1), 515–520.
- Ravindiran G., Jeyaraju R.M., Josephraj J., and Alagumalai A. (2019). Comparative desorption studies on remediation of remazol dyes using biochar (Sorbent) derived from green marine seaweeds. *ChemistrySelect*, **4**(25), 7437–7445.
- Saini A.S., and Melo J.S. (2013). Biosorption of uranium by melanin: Kinetic, equilibrium and thermodynamic studies. *Bioresource Technology*, **149** 155–162.
- Sampranpiboon P., and Charnkeitkong P. (2010). Equilibrium Isotherm, Thermodynamic and Kinetic Studies of Lead adsorption onto pineapple and paper waste sludges. *International Journal of Energy and Environment*, **4**(3).
- Sowmya A., and Meenakshi S. (2013). An efficient and regenerable quaternary amine modified chitosan beads for

the removal of nitrate and phosphate anions. *Journal of Environmental Chemical Engineering*, **1**, 906–915.

Sujatha S, Gokulan R., Zunaithur Rahman D.R. and Yogeshwaran V. (2022). "Investigation of Mechanism of Metal Ion Adsorption from Aqueous Solutions using *Prosopis Julyflora* Roots: Batch and Fixed Bed Column Studies", Global NEST, March 2022.

Unnithan M.R., and Anirudhan T.S. (2001). The Kinetics and Thermodynamics of Sorption of Chromium(VI) onto the Iron(III) Complex of a Carboxylated Polyacrylamide-Grafted Sawdust. *Industrial & Engineering Chemistry Research*, **40**, 2693–2701.

Xiong M.X., Yang M., Chen Q.L., Cai T.Y. (August 2022). Mechanism studies for adsorption and extraction of soluble sodium from bauxite residue: Characterization, kinetics, and thermodynamics. *Chemical Engineering*, **10**(4), 108183.

Zogorski J.S. (1976). Samuel Denton Faust and J. Haas. "The kinetics of adsorption of phenols by granular activated carbon.